The American Journal of Pathology, Vol. 174, No. 4, April 2009

DOI: 10.2353/ajpath.2009.080816

Tumorigenesis and Neoplastic Progression

Regulation of Prostate Cancer Progression by Galectin-3

Yi Wang,* Pratima Nangia-Makker,* Larry Tait,† Vitaly Balan,* Victor Hogan,* Kenneth J. Pienta,‡§ and Avraham Raz*

From the Tumor Progression and Metastasis and Breast Cancer Program,† Karmanos Cancer Institute, School of Medicine, Wayne State University, Detroit; and the Departments of Internal Medicine‡ and Urology,§ University of Michigan, Ann Arbor, Michigan*

Galectin-3, a β-galactoside-binding protein, has been implicated in a variety of biological functions including cell proliferation, apoptosis, angiogenesis, tumor progression, and metastasis. The present study was undertaken to understand the role of galectin-3 in the progression of prostate cancer. Immunohistochemical analysis of galectin-3 expression revealed that galectin-3 was cleaved during the progression of prostate cancer. Galectin-3 knockdown by small interfering RNA (siRNA) was associated with reduced cell migration, invasion, cell proliferation, anchorage-independent colony formation, and tumor growth in the prostates of nude mice. Galectin-3 knockdown in human prostate cancer PC3 cells led to cell-cycle arrest at G_1 phase, up-regulation of nuclear p21, and hypophosphorylation of the retinoblastoma tumor suppressor protein (pRb), with no effect on cyclin D1, cyclin E, cyclin-dependent kinases (CDK2 and CDK4), and p27 protein expression levels. The data obtained here implicate galectin-3 in prostate cancer progression and suggest that galectin-3 may serve as both a diagnostic marker and therapeutic target for future disease treatments. ***(Am J Pathol 2009, 174:1515–1523; DOI: 10.2353/ajpath.2009.080816)***

Prostate cancer is the second most common lethal malignancy in American men.[1–3] Prostate cancer has posed a major public health problem in the United States and worldwide.[4,5] There is a continuous search for better diagnostic markers and therapeutic targets for this disease. Galectin-3 is a β-galactoside-binding protein that binds to the carbohydrate portion of cell surface glycoproteins or glycolipids.[6,7] It is comprised of three distinct structural domains: a short NH_2-terminal domain containing a serine phosphorylation site, a repeated collagen α-like sequence, and a COOH-terminal domain containing a single carbohydrate recognition-binding domain.[8,9] The collagen α-like sequence contains a cleavage site at the Ala^{62}-Tyr^{63} peptide bond for matrix metalloproteinases (MMP-2 and MMP-9).[10] Expression of galectin-3 is related to malignant transformation of many types of tumors.[11–13] In human prostate cancer, galectin-3 expression was reported to be down-regulated with progressive stages,[14–17] whereas in many other cancers such as thyroid, gastric carcinoma, and squamous cell carcinoma of the head and neck, galectin-3 expression was up-regulated with increased malignant phenotype.[18–20] Recently, *in vivo* cleavage of galectin-3 was reported in breast cancer using two specific antibodies: a monoclonal antibody that recognizes intact galectin-3 and a polyclonal antibody that recognizes both intact and cleaved galectin-3. Cleaved galectin-3 co-localized with active MMP-2/MMP-9 in mouse xenografts and human breast cancer tissues, indicating that cleavage of galectin-3 is attributable to MMPs.[21] Because cleaved galectin-3 is recognized by the polyclonal antibody, but not the monoclonal antibody, we questioned if previous studies on galectin-3 expression in human prostate cancer using a single antibody provided the complete picture of the significance of this protein in prostate cancer. In this study, we evaluated the role of galectin-3 during the progression of human prostate cancer using two approaches: staining human prostate cancer tissues with differential antibodies and silencing galectin-3 expression in human prostate cancer PC3 cells with siRNA.

Supported by the National Institutes of Health (grants R37CA46120-19 to A.R. and P50 CA69568 to K.P.), the Karmanos Cancer Institute (strategic research grant to A.R. and P.N.-M.), and the American Cancer Society (clinical research professor to K.J.P.).

Accepted for publication January 2, 2009.

Address reprint requests to Avraham Raz, Ph.D., Tumor Progression and Metastasis, Karmanos Cancer Institute, School of Medicine, Wayne State University, 110 East Warren Ave., Detroit, MI 48201. E-mail: raza@karmanos.org.

Materials and Methods

Antibodies

Customized polyclonal rabbit anti-galectin-3 antibody against the recombinant whole molecule was created by Zymed Laboratories (South San Francisco, CA). Monoclonal rat anti-galectin-3 antibody was isolated from the supernatant of hybridoma (catalogue no. TIB-166; American Type Culture Collection, Rockville, MD). Monoclonal mouse anti-MMP-2 and anti-MMP-9 antibodies were purchased from Calbiochem (San Diego, CA). Monoclonal mouse anti-Cip1 antibody was purchased from Transduction Laboratories (Lexington, KY). Monoclonal mouse anti-cyclin E and anti-p27 were purchased from BD Biosciences (San Diego, CA). Polyclonal rabbit anti-CDK2 and anti-CDK4 antibodies were from Santa Cruz Biotechnology (Santa Cruz, CA). Polyclonal rabbit anti-phosphopRb and anti-lamin A/C antibodies were from Cell Signaling Technology (Beverly, MA). Monoclonal mouse anti-cyclin D1, anti-β-actin, and anti-β-tubulin antibodies were purchased from Sigma Chemicals (St. Louis, MO).

Immunohistochemical Analysis

A prostate cancer tissue array including normal prostate tissues (n = 30), prostate intraepithelial neoplasia (n = 30), Gleason 3 and 4 cancer tissues (n = 82), and metastatic lesions (n = 26) was constructed at the University of Michigan Prostate Specialized Program of Research Excellence Tissue Core. It was deparaffinized, rehydrated, and boiled in 1 mmol/L sodium citrate buffer (pH 6.0) by microwave for 10 minutes. Endogenous peroxidase activity was blocked by 0.3% hydrogen peroxide, and nonspecific binding of immunoglobulin was minimized by blocking with Super Block (Skytek Laboratories, Logan, UT) for 1 hour at room temperature. Sections were incubated with anti-galectin-3 antibodies (1:500 for polyclonal, 1:100 for monoclonal) overnight at 4°C, then linked with appropriate biotinylated secondary antibodies (1:500; Vector Laboratories, Burlingame, CA) for 1 hour and the avidin-biotin-peroxidase complex for 30 minutes at room temperature, colorized by 3′-3′-diaminobenzidine tetrachloride (Sigma Chemicals) and counterstained with hematoxylin. Visualization and documentation were accomplished with an Olympus (Melville, NY) BX40 microscope supporting a Sony (Tokyo, Japan) DXC-979MD 3CCCD video camera. Results were evaluated by two investigators in blinded manner. Galectin-3 immunostaining was evaluated by the percentage of positively stained epithelial cells in each section. Sections with more than 10% of positive cancer cells are regarded as positive samples.

Cell Culture

Human prostate cancer PC3 cells (American Type Culture Collection CRL-1435) were purchased from the American Type Culture Collection. PC3 cells and siRNA-transfected clones were cultured in Dulbecco's modified Eagle's medium (DMEM) supplemented with 10% fetal bovine serum (FBS), 100 U/ml penicillin, and 100 μg/ml streptomycin. Cultures were maintained at 37°C in a 5% CO_2 humidified incubator. For collection of conditioned medium the cells were grown for 24 hours in basic DMEM without the supplements.

RNA Interference

Small interfering oligonucleotides targeting human galectin-3 gene (5′-GATCCCGGGAAGAAAGACAGTCGGTTTCAAGAGAACCGACTGTCTTTCTTCCCTTTTTTGGAAA-3′) and its complement were synthesized and annealed by Thermo Scientific (Pittsburgh, PA). It was subcloned into pSilencer 3.1-H1 neo expression vector (Ambion, Austin, TX) between *Bam*HI and *Hind*III sites to construct pSilencer 3.1-H1/siGal3-producing siRNA targeting galectin-3 mRNA. PC3 cells were transfected with this constructed vector and pSilencer 3.1-H1-negative control vector containing a random sequence insert using Lipofectamine 2000 reagent (Invitrogen, Carlsbad, CA) according to the manufacturer's instructions. Stable clones were selected by 600 μg/ml of G418 (Invitrogen).

Reverse Transcriptase-Polymerase Chain Reaction (RT-PCR) Analysis

Total RNA was extracted with Trizol reagent (Invitrogen). Two μg of total RNA was used for the RT reaction (20 μl total volume) by using the First-Strand cDNA synthesis kit (GE Healthcare, Piscataway, NJ) according to the manufacturer's instruction. One μl of the resultant cDNA from the RT reaction was used as the template in PCR reactions. PCR conditions were as follows: 95°C for 3 minutes, followed by 24 cycles of 95°C for 40 seconds, 55°C for 30 seconds, and 72°C for 1 minute, the final extension was at 72°C for 5 minutes. The following primers were used: 5′-GCCACTGATTGTGCCTTA-3′ (forward) and 5′-AACCGACTGTCTTTCTTCC-3′ (reverse) for human galectin-3 gene; 5′-TCAACGGATTTGGTCGTATT-3′ (forward) and 5′-TTGGCAGGTTTTTCTAGACG-3′ (reverse) for human glyceraldehyde 3-phosphate dehydrogenase (GAPDH) gene. PCR products were electrophoresed on 1% agarose gel and stained with ethidium bromide. Density of each band was quantitated using ImageJ software (National Institutes of Health, Bethesda, MD) and band intensity of galectin-3 was standardized to that of GAPDH.

Western Blot Analysis

Cells were lysed in RIPA buffer (1% sodium deoxycholate, 0.1% sodium dodecyl sulfate, 1% Triton X-100, 1% bovine hemoglobin, 1 mmol/L iodoacetamide, 10 mmol/L Tris-HCl, pH 8.0, 140 mmol/L sodium chloride, 0.025% sodium azide) containing 1 mmol/L phenylmethyl sulfonyl fluoride, 1 μmol/L leupeptin, 1 μmol/L pepstatin, and 1 μmol/L aprotinin. Protein concentration was determined using a protein assay reagent (Bio-Rad, Hercules, CA). Equal amounts of proteins were separated on sodium dodecyl sulfate-polyacrylamide gel electrophore-

sis gels and transferred to polyvinylidene fluoride membranes (Millipore, Bedford, MA). Membranes were blocked in 0.1% casein/0.2× phosphate-buffered saline (PBS) for 1 hour, incubated with appropriate primary antibodies (rabbit anti-galectin-3, 1:1000; mouse anti-MMP-2 and anti-MMP-9, 1:800; mouse anti-Cip1, 1:250; mouse anti-p27, 1:500; mouse anti-cyclin E, 1:500; rabbit anti-CDK2 and anti-CDK4, 1:300; mouse anti-cyclin D1, 1:400; rabbit anti-phospho-pRb, 1:1000; rabbit anti-lamin A/C, 1:1000; mouse anti-β-actin and anti-tubulin, 1:5000) for 2 hours, then incubated with appropriate secondary antibodies conjugated with IRDye 800 (Rockland Immunochemicals, Gilbertsville, PA) or Alexa Fluor 680 (Invitrogen) for 40 minutes. After incubation of primary and secondary antibodies, membranes were washed four times with TPBS (PBS with 0.1% Tween 20) at 5-minute intervals. Immunoblots were visualized using the Odyssey infrared imaging system (LI-COR Biosciences, Lincoln, NE). Density of each band was quantitated by ImageJ software.

Cell Migration Assay

Cell migration was measured using a chemotaxis chamber (Neuro Probe, Cabin John, MD). Briefly, basic DMEM containing chemoattractants (0.05 mg/ml laminin or 0.1 mg/ml Matrigel) was added to the lower chamber. Cells suspended in basic DMEM were added to the upper chamber and incubated for 5 hours at 37C. The two chambers were separated by polycarbonate filters (8-μm pore size). At the end of incubation, cells on the top side of the filter were wiped off, cells that migrated to the lower surface of the filter were fixed and stained with the Diff-Quik stain set (Fisher Scientific, Pittsburgh, PA). Quantification was performed by counting the stained cells under a microscope.

Cell Invasion Assay

Cell invasion assay was performed using the Matrigel invasion chamber (BD Biosciences). Briefly, basic DMEM containing chemoattractant (0.05 mg/ml laminin) was added to the chambers and cells suspended in basic DMEM were seeded into the inserts. After 17 hours of incubation, noninvading cells on the upper side of the inserts were removed using a cotton swab, invading cells on the bottom side of the inserts were fixed and stained with the Diff-Quik stain set. Quantification was performed by counting the stained cells under a microscope.

Gelatin Zymography

Conditioned media were concentrated using Amicon Ultra centrifugal filter devices (Millipore) and protein concentration was determined using Bio-Rad protein assay reagent. Ten μg of concentrated supernatants were separated on a 8% sodium dodecyl sulfate-polyacrylamide gel electrophoresis gel containing 1 mg/ml of gelatin. The gel was washed three times with 2.5% Triton X-100 for 10 minutes, and 10 mmol/L Tris-HCl (pH 8.0) for 10 minutes each. Then, the gel was incubated in 50 mmol/L Tris-HCl (pH 8.0) with 5 mmol/L $CaCl_2$ for 16 hours at 37°C and stained with 1% Coomassie Brilliant Blue solution. After destaining, sharp transparent bands indicating gelatinolytic activity were visualized in blue background. Density of each band was quantified with ImageJ software.

Cell Growth Assay

Cell growth was evaluated by 3-(4,5)-dimethylthiahiazo(-z-y1)-3,5-di-phenytetrazoliumromide (MTT). Briefly, 1×10^4 cells/well were plated in 96-well plates and cultured for 5 days. Fresh DMEM/10% FBS was replaced on the third day. Each day, 20 μl of MTT (5 mg/ml) in 200 μl of basic DMEM per well were added to one set and incubated for 4 hours. After removing MTT, 200 μl of dimethyl sulfoxide were added and mixed vigorously. Absorbance was measured at 490 nm using a V_{max} microplate reader (Molecular Devices, Sunnyvale, CA). Absorbance was converted to cell number using a standard curve prepared by precounted cells.

Cell-Cycle Analysis

Cells were plated at a density of 1×10^6 cells/dish in 10-cm culture dishes, incubated in DMEM/0.2% FBS for 24 hours, then another 24 hours in DMEM/10% FBS. Aliquots of 1×10^6 cells were fixed in 70% ethanol at −20°C for 24 hours. Fixed cells were washed with PBS and suspended in 500 μl of propidium iodide/Triton X-100/RNase staining solution for 15 minutes at 37°C in the dark. Cell-cycle analysis was performed using FACSCalibur flow cytometer (BD Biosciences).

Immunofluorescence

Cells were fixed with 4% paraformaldehyde/PBS for 15 minutes, permeabilized with 0.2% Triton X-100/PBS for 10 minutes, blocked in 1% bovine serum albumin/PBS for 30 minutes, and incubated with monoclonal mouse-anti-Cip1 antibody (1:100) for 1 hour, then incubated with Texas Red-conjugated anti-mouse antibody (1:2000; ICN Biomedicals, Costa Mesa, CA) for 1 hour in the dark. After each antibody treatment, cells were washed three times with 0.1% bovine serum albumin/PBS for 5 minutes each. Next, cells were stained with 4′,6-diamidino-2-phenylindole for 3 minutes, washed three times with double-distilled water for 5 minutes, and mounted on a glass slide with 80% glycerol. Fluorescent images were acquired using a color Sony camera connected to a fluorescence Olympus microscope.

Preparation of Nuclear Extracts

Cells were washed with ice-cold PBS twice, trypsinized, and centrifuged at 500 × *g* for 5 minutes. The supernatant was discarded and the cell pellet was used for extraction of the nuclear and cytoplasmic fractions using NE-PER nuclear and cytoplasmic extraction reagents

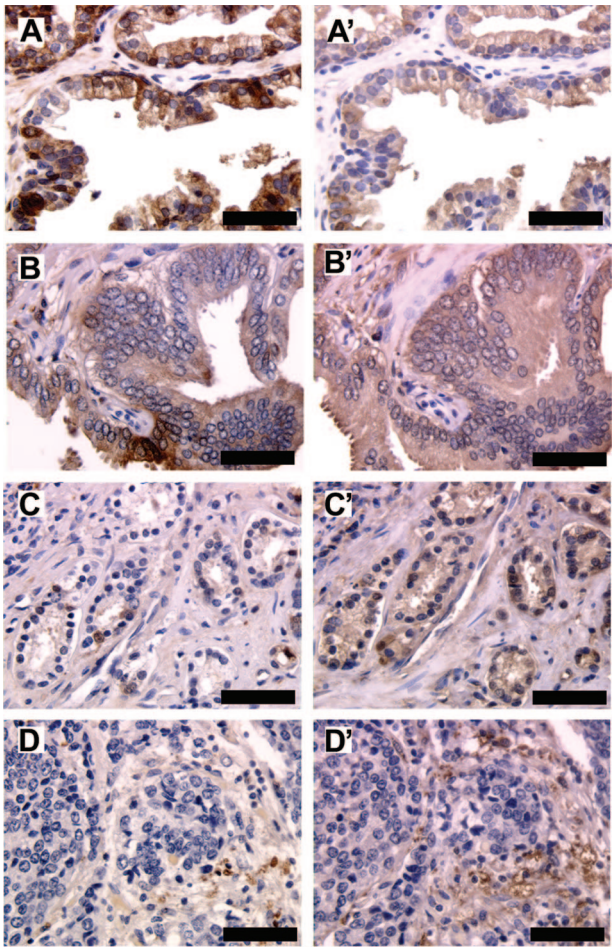

Figure 1. Cleavage of galectin-3 in prostate cancer progression. A prostate cancer tissue array was stained for intact and cleaved galectin-3 using monoclonal and polyclonal anti-galectin-3 antibodies, respectively. **A–D:** Monoclonal anti-galectin-3 antibody. **A'–D':** Polyclonal anti-galectin-3 antibody. **A** and **A':** Normal prostate tissue. **B** and **B':** Prostate intraepithelial neoplasia. **C** and **C':** Gleason 3 cancer tissue. **D** and **D':** Metastatic lesion. Scale bars = 150 μm.

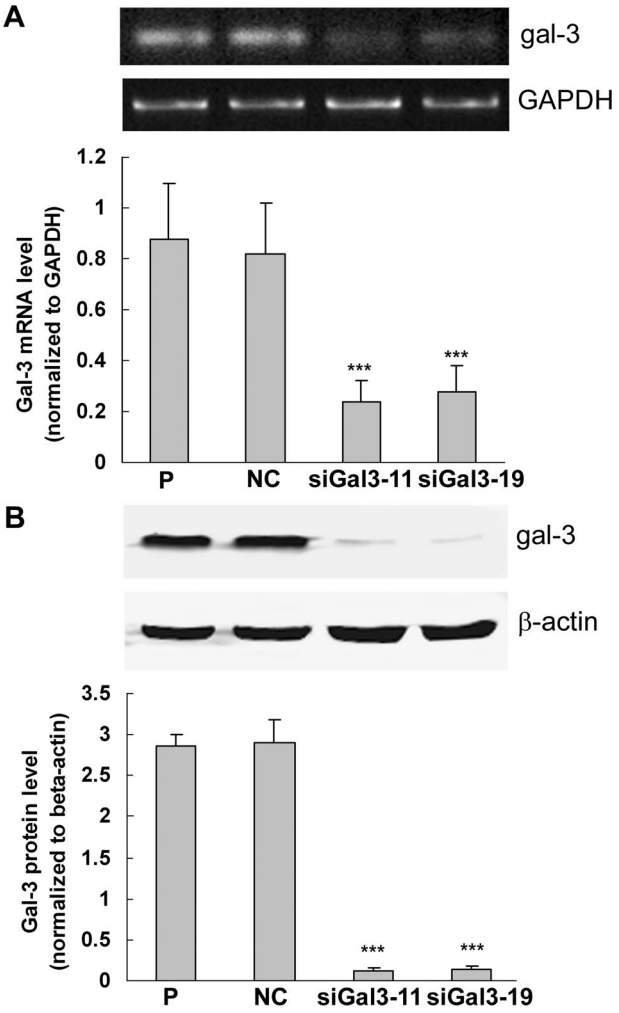

Figure 2. Down-regulation of galectin-3 expression by siRNA in PC3 cells. **A: Top:** RT-PCR analysis of galectin-3 mRNA levels in knockdown clones and control cells. GAPDH was used as the loading control. **A: Bottom:** Quantification of galectin-3 mRNA levels normalized to GAPDH. **B: Top:** Western blot analysis of galectin-3 protein levels. β-Actin was used as the loading control. **B: Bottom:** Quantification of galectin-3 protein levels normalized to β-actin. Results are representative of three independent experiments. $^{***}P < 0.001$, compared with control cells. P, parental cells; NC, negative control; siGal3-11 and siGal3-19, knockdown clones.

(Pierce Biotechnology, Rockford, IL) according to the manufacturer's instructions.

Anchorage-Independent Growth Assay

Six-well plates were coated with 1% SeaPlaque agarose (BioWhittaker Molecular Applications, Rockland, ME) dissolved in DMEM/10% FBS. Cells (1×10^3) suspended in DMEM/10% FBS containing 0.5% agarose were overlaid on the bottom layer. The plates were kept at 4°C for 2 hours, then moved to a tissue culture incubator. Twenty-four hours later, fresh DMEM/10% FBS was placed on top and replaced every 3 days. Colonies were counted 3 weeks later and photographed using phase-contrast photomicrography. Colonies measuring 0.1 mm or greater in diameter were scored. Results were expressed as the percentage of colonies in total number of seeded cells.

Tumorigenesis in Nude Mice

To determine tumorigenesis *in vivo*, orthotopic implantation was performed in athymic male nude mice (nu/nu, 10 to 12 weeks old) obtained from Taconic (Germantown, NY). Animal handling and experimental procedures were approved by the Animal Investigation Committee of Wayne State University. After total body anesthesia with ketamine (70 mg/kg) and xylazine (7.5 mg/kg), a midline incision was made in the lower abdomen and the seminal vesicles were carefully retracted with a sterile cotton swab. Cells (1×10^6 in 20 μl of PBS) were injected into the ventral lobe of the prostate using a 30-gauge needle attached to a 500-μl syringe. The abdomen was closed by single-stitch sutures using 5–0 Dexon II (Covidien, Mansfield, MA) absorbable polyglycolic acid suture. Eight mice were used per group. Mice were sacrificed after 30 days. The primary tumors were excised, weighed, and photographed.

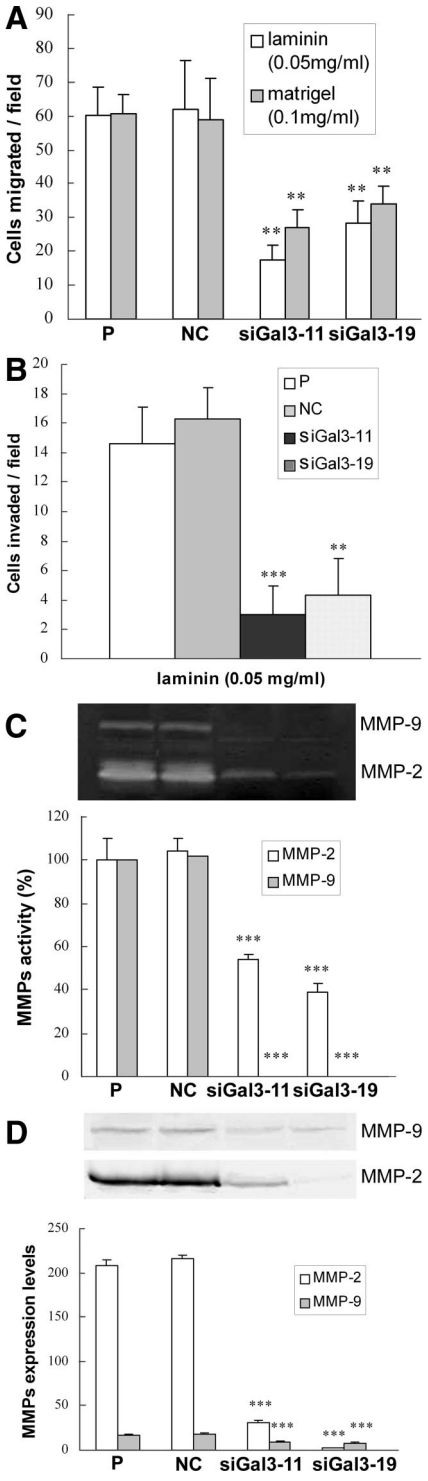

Figure 3. Cell migration and invasion of galectin-3 knockdown PC3 cells. **A:** Chemotaxis assay. Fifty μg/ml of laminin and 100 μg/ml of Matrigel were used as chemoattractants. **B:** Chemoinvasion through Matrigel. Fifty μg/ml of laminin were used as the chemoattractant. **C: Top:** Gelatin zymography. **D: Top:** Western blot analysis. **C** and **D: Bottom:** Quantification of activity and expression levels of MMP-2 and MMP-9, respectively. Results are representative of three independent experiments. $^{**}P < 0.01$; $^{***}P < 0.001$, compared with control cells.

Statistical Analysis

The χ^2 test, Fisher's exact test, and paired *t*-test were used for statistical analysis of immunohistochemistry staining. Data from other experiments are expressed as mean ± SD of three independent experiments. Comparisons between the groups were determined by using one-way analysis of variance test. $P < 0.05$ was considered statistically significant. All data were analyzed with SPSS 14.0 (Chicago, IL).

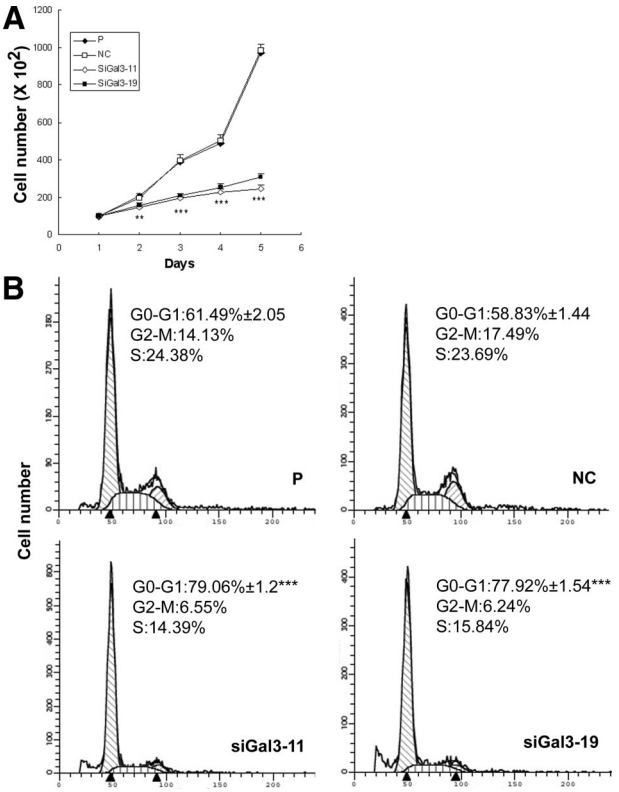

Figure 4. Cell growth and cell-cycle analysis in galectin-3 knockdown clones. **A:** Cell growth analyzed by MTT assay. **B:** Cell-cycle analysis showed a higher percentage of cells in G_1 phase in knockdown clones. Results are representative of three independent experiments. $^{**}P < 0.01$; $^{***}P < 0.001$, compared with control cells.

Results

Cleavage of Galectin-3 in Human Prostate Cancer

To understand the alteration of galectin-3 expression in human prostate cancer, we examined the percentage of positively stained epithelial cells in each section by two different antibodies as described.[21] As shown in Figure 1 A, A', B, and B', galectin-3 was detected mainly in the cytoplasm of epithelial cells in all of the samples. Even though the intensity of staining was weaker using the polyclonal antibody, both the antibodies depicted a similar percentage of galectin-3-positive cells, indicating that galectin-3 is not cleaved in either normal prostate or prostate intraepithelial neoplasia. In the case of Gleason 3 and 4 cancer tissues, the polyclonal antibody detection showed 57% positive samples (47 of 82) and 43% negative samples (35 of 82), whereas monoclonal antibody detection showed 22% positive samples (18 of 82) and 78% negative samples (64 of 82) ($\chi^2 = 21.4$, $v = 1$, $P <$

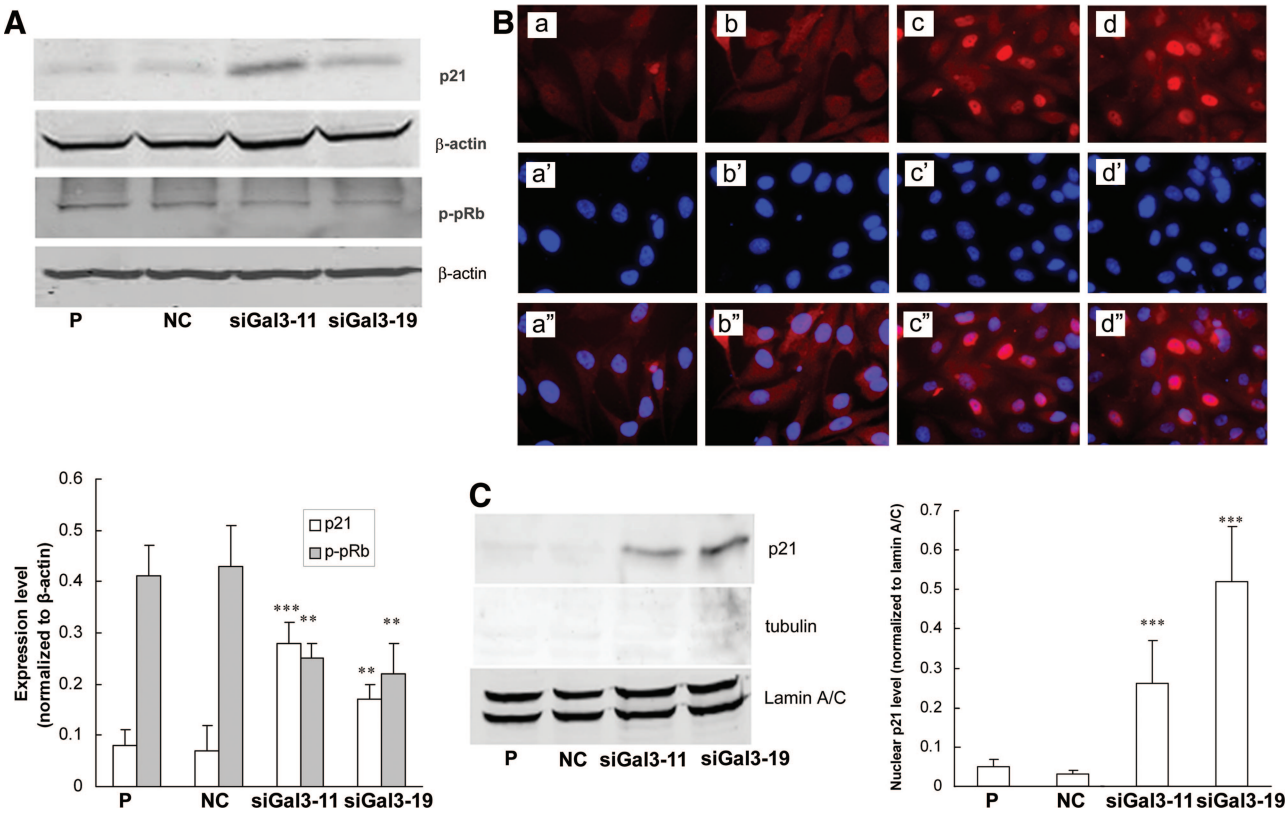

Figure 5. Up-regulation and nuclear transport of p21 in galectin-3 knockdown clones. **A: Top:** Galectin-3 knockdown increased p21 expression and suppressed phosphorylation of pRb in total cell lysate. β-Actin was used as the loading control. **A: Bottom:** Quantification of expressions of p21 and p-pRb normalized to β-actin. **B:** Expression of p21 by immunofluorescence assay. **a–d:** p21 staining. **a'–d':** Nuclear staining by 4′,6-diamidino-2-phenylindole. **a"–d":** Merged pictures. **a–a":** Parental. **b–b":** Negative control. **c–c":** siGal3-11. **d–d":** siGal3-19. **C: Left:** Western blot analysis of p21 expression in nuclear extracts. Tubulin was used as the marker of cytoplasmic extracts. Lamin A/C was used as the marker of nuclear extracts. **C: Right:** Quantification of nuclear p21 expression normalized to lamin A/C. Results are representative of three independent experiments. $^{**}P < 0.01$; $^{***}P < 0.001$, compared with control cells. Original magnifications, ×40.

0.001) (Figure 1, C and C'). These 22% of the samples were positive for both the antibodies. Within these samples, most of the sections displayed 65 to 90% positive cells as detected by polyclonal antibody, whereas 10 to 50% positive cells were detected by monoclonal antibody. To analyze the galectin-3 cleavage in these samples, paired *t*-test was applied to compare the percentage of positive cells using the two antibodies ($T = 5.46$, $P < 0.001$). A higher number of sections that are positive for polyclonal antibody and a higher number of positive cells within each section indicate that galectin-3 is cleaved in Gleason 3 and 4. In case of metastatic lesions, 23% of the samples were positive for cleaved galectin-3 and 12% of the samples were positive for intact galectin-3 (Figure 1, D and D'). These data suggested that galectin-3 cleavage occurred during the malignant transformation and progression of human prostate cancer.

Galectin-3 Knockdown in PC3 Cells by RNAi

PC3 cells were transfected with pSilencer 3.1-H1/siGal3 and pSilencer 3.1-H1-negative control vector. After G418 selection and screening by Western blot, one negative control clone (NC) and two galectin-3 knockdown clones (siGal3-11 and siGal3-19) were selected for the subsequent experiments. As shown in Figure 2A, galectin-3 mRNA levels in siGal3-11 and siGal3-19 were reduced by 73% and 68%, respectively, compared with control cells. Figure 2B showed that expression levels of galectin-3 protein in siGal3-11 and siGal3-19 were reduced by ~90%.

Galectin-3 Knockdown Suppressed Cell Migration, Invasion, and Activities of MMP-2/MMP-9 in PC3 Cells

The effects of galectin-3 knockdown on cell migration and invasion were evaluated by chemotaxis and Matrigel invasion assays, respectively. Chemotaxis of siGal3-11 and siGal3-19 was reduced to 28% and 46%, respectively, toward laminin and 44% and 56%, respectively, toward Matrigel of that in control cells (Figure 3A). Compared with control cells, galectin-3 knockdown clones showed a significant reduction of invasive capacity toward laminin (Figure 3B). Activity levels of MMP-2 in siGal3-11 and siGal3-19 clones were dramatically decreased to 54% and 39%, respectively, of that in control cells; activity levels of MMP-9 in galectin-3 knockdown clones were almost completely suppressed as indicated by gelatin zymography (Figure 3C). Western blot analysis of conditioned media confirmed the zymography results (Figure 3D). Galectin-3 knockdown had no effects on

expression levels of pro-MMP-2 and pro-MMP-9 in total cell lysate (data not shown).

Galectin-3 Knockdown Inhibited Cell Growth and Induced Cell-Cycle Arrest at G_1 Phase

The MTT assay was used to investigate the effect of galectin-3 knockdown on the growth of PC3 cells. The two galectin-3 knockdown clones showed slower cell growth rate compared with control cells (Figure 4A). To analyze the reason for reduced cell growth, cell-cycle distribution was determined by flow cytometry analysis. As shown in Figure 4B, 79% of siGal3-11 cells and 78% of siGal3-19 cells were distributed in G_1 phase, whereas, only 61% of parental cells and 59% of negative control cells remained in G_1 phase, which suggested galectin-3 knockdown induced cell-cycle arrest at G_1 phase.

Up-Regulation of Nuclear p21 Contributes to G_1 Cell-Cycle Arrest

To explore the underlying mechanism of cell-cycle arrest by galectin-3 knockdown, expression of cell-cycle-related proteins (cyclin D_1, cyclin E, CDK2, CDK4, p21, p27, and pRb) in total cell lysate were examined by Western blot analysis. The two knockdown clones showed up-regulation of p21 and hypophosphorylation of pRb (Figure 5A). Galectin-3 knockdown had no effect on expression of cyclin D_1, cyclin E, CDK2, CDK4, or p27 (data not shown). It was reported that p21 exerts inhibitory effects on cell-cycle transition only when it is localized in the nucleus.[22] Therefore, immunofluorescence staining and Western blot analysis were performed to detect nuclear p21. Figure 5B showed an intense signal of nuclear p21 in two knockdown clones. Western blot analysis also showed an up-regulation of nuclear p21 in siGal3-11 and siGal3-19 clones (Figure 5C).

Galectin-3 Knockdown Inhibited Tumorigenicity of PC3 Cells

The role of galectin-3 knockdown in tumorigenesis was evaluated by anchorage-independent growth in soft agar and tumor growth in nude mice. As shown in Figure 6A, the colonies of galectin-3 knockdown cells were smaller than that of controls, and colony-forming efficiency of siGal3-11 and siGal3-19 were reduced to 19% and 31% of that in control cells, respectively. Orthotopic implantation of two knockdown clones or negative control cells were performed in nude mice. Mean tumor weights of galectin-3 knockdown clones were significantly reduced compared with negative control cells at 30 days (Figure 6B).

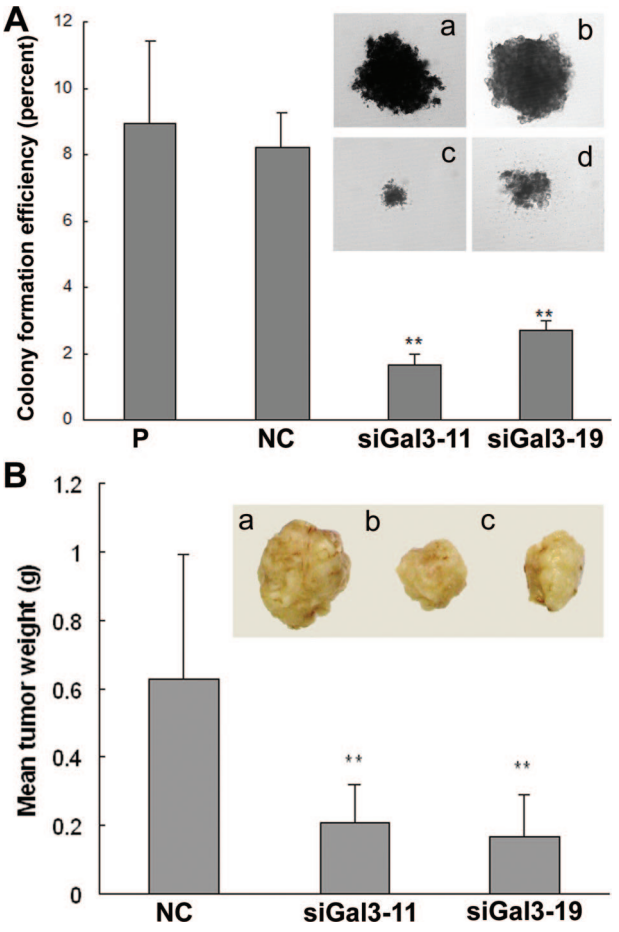

Figure 6. Galectin-3 knockdown inhibited tumorigenicity of PC3 cells. **A:** Tumorigenicity *in vitro* was analyzed by anchorage-independent growth assay. Compared with controls, colony formation rate in knockdown clones were reduced. **Inset:** Size of the soft agar colonies. **a:** Parental. **b:** Negative control. **c:** siGal3-11. **d:** siGal3-19. Results are representative of three independent experiments. **B:** Mean tumor weight in galectin-3 knockdown clones was less than that in negative control. **Inset:** Representative picture of tumors. **a:** Negative control. **b:** siGal3-11. **c:** siGal3-19. $^{**}P < 0.01$, compared with control cells. Original magnifications, ×10.

Discussion

A growing body of literature describes the correlation of galectin-3 protein expression with neoplastic progression. High expression levels of galectin-3 have been detected in papillary carcinoma of the thyroid, squamous cell carcinoma of the head and neck, and primary and metastatic gastric carcinoma. In contrast, galectin-3 down-regulation has been reported during the progression of cancers of the breast, uterus, and ovary.[23,24] Furthermore, redistribution/relocalization of galectin-3 was reported in breast, colon, and prostate cancers.[25,26] In human prostate cancer, a decreased expression of galectin-3 during the progression was reported using a monoclonal antibody recognizing only an intact (non-cleaved) galectin-3.[14–17] However, because galectin-3 is a substrate for MMPs and is cleaved *in vivo* during breast cancer progression,[21] we questioned whether cleavage of galectin-3 might be also a part of prostate cancer progression and could be detected in biopsies. A human prostate cancer tissue array was analyzed by immunohistochemistry using two differential anti-galectin-3 antibodies. We found that the percentage and distribution of positive stained cells detected by both of the antibodies was similar in all of the normal or prostate intraepithelial neoplasia tissue samples, which indicates that no cleav-

age occurred in these two stages. However, in Gleason 3 and 4 cancer tissues, a significantly higher percentage of positive samples and more galectin-3-positive cells in the same section were detected using polyclonal antibody compared with the monoclonal antibody, indicating cleavage of galectin-3. Our data demonstrated that galectin-3 is cleaved during the malignant transformation of human prostate cancer, which suggested that cleavage of galectin-3, not just the presence of intact galectin-3, could be used as the maker for diagnosis of prostate cancer.

To date, the actual biological functions of galectin-3 in prostate cancer have not been well described. In this study, we down-regulated galectin-3 protein expression to 10% of that in control cells and investigated its effects on the biological behavior of PC3 cells. Our data showed that galectin-3 knockdown in PC3 cells contributed to reduced cell migration, cell invasion, and suppression of MMP-2 and MMP-9, which suggested the association of galectin-3 with metastatic events of PC3 cells. Our data are consistent with the observations in many other human cancers such as breast, colon, and brain tumors.[27–29]

Significant evidence has shown that galectin-3 is implicated in modulation of tumor cell growth. Human leukemia T cells transfected with galectin-3 displayed higher growth rates than control nonexpressing transfectants.[31] Inhibition of galectin-3 gene expression in human pituitary adenoma cells HP75 resulted in decreased cell proliferation.[31] After treatment with modified citrus pectin, a natural inhibitor of galectin-3, human prostatic cancer cells JCA-1 displayed reduced ^{3}H-thymidine incorporation into DNA and cell growth.[32] In the present study, galectin-3 knockdown in prostate cancer cells PC3 reduced cell growth and induced cell-cycle arrest at the G_1 phase. The G_1 cell-cycle arrest seemed to be attributable to up-regulation of p21 expression and its nuclear localization, moreover, downstream pRb displayed hypophosphorylation that inhibits the transcription of genes required to traverse G_1 to S phase.

A relationship of galectin-3 expression with tumorigenic phenotype of many cancer cells has been demonstrated. Introduction of galectin-3 cDNA into galectin-3-null human breast cancer cells BT-549 resulted in the acquisition of tumorigenicity of BT549 cells in nude mice.[33] Inhibition of galectin-3 expression in highly malignant human breast carcinoma cells MDA-MB-435 led to the abrogation of anchorage-independent growth and a significant suppression of tumor growth in nude mice.[34] Similar data were reported for fibroblasts[35] and LS174T colon carcinoma cells.[28] Ellerhorst and colleagues[36] reported that LNCaP cells, which do not constitutively express galectin-3 did not show a statistically significant difference in the tumor-forming potential when transfected with galectin-3. Among the tumors that developed from galectin-3 lines, however, only 1 of 24 was found to have glaectin-3-positive cells. Based on these results, it is difficult to interpret the role of galectin-3 in tumorigenicity of LNCaP cells. We have shown here that galectin-3 knockdown PC3 cells displayed reduced colony size and efficiency of colony formation in soft agar. Loss of galectin-3 expression also resulted in reduced tumor growth when cells were injected in the ventral prostate of nude mice. Taken together with observations in other tumor types, it could be postulated that galectin-3 expression is associated with maintenance of tumorigenic potential of cancer cells.

In conclusion, the data show that galectin-3 is cleaved during the progression of prostate cancer and might be associated with metastasis, cell growth, and tumorigenicity of PC3 cells. Expression of intact versus cleaved galectin-3 thus might be used as a marker for prognosis of prostate cancer and a therapeutic target for the treatment of prostate cancer.

Acknowledgments

We thank Drs. Susuma Nakahara, Tatsuyoshi Funasaka, and Huankai Hu for their kind help in the experiments; and Vivian Powell for her help in submission of the manuscript.

References

1. Zhang X, Jin TG, Yang H, DeWolf WC, Khosravi-Far R, Olumi AF: Persistent c-FLIP(L) expression is necessary and sufficient to maintain resistance to tumor necrosis factor-related apoptosis-inducing ligand-mediated apoptosis in prostate cancer. Cancer Res 2004, 64:7086–7091
2. Shah RB, Mehra R, Chinnaiyan AM, Shen R, Ghosh D, Zhou M, Macvicar GR, Varambally S, Harwood J, Bismar TA, Kim R, Rubin MA, Pienta KJ: Androgen-independent prostate cancer is a heterogeneous group of diseases: lessons from a rapid autopsy program. Cancer Res 2004, 64:9209–9216
3. Jemal A, Murray T, Samuels A, Ghafoor A, Ward E, Thun MJ: Cancer statistics, 2003. CA Cancer J Clin 2003, 53:5–26
4. Zhang Z, Li M, Wang H, Agrawal S, Zhang R: Antisense therapy targeting MDM2 oncogene in prostate cancer: effects on proliferation, apoptosis, multiple gene expression, and chemotherapy. Proc Natl Acad Sci USA 2003, 100:11636–11641
5. Boyd DD, Kim SJ, Wang H, Jones TR, Gallick GE: A urokinase-derived peptide (A6) increases survival of mice bearing orthotopically grown prostate cancer and reduces lymph node metastasis. Am J Pathol 2003, 162:619–626
6. Woo HJ, Shaw LM, Messier JM, Mercurio AM: The major non-integrin laminin binding protein of macrophages is identical to carbohydrate binding protein 35 (Mac-2). J Biol Chem 1990, 265:7097–7099
7. Cherayil BJ, Chaitovitz S, Wong C, Pillai S: Molecular cloning of a human macrophage lectin specific for galactose. Proc Natl Acad Sci USA 1990, 87:7324–7328
8. Barondes SH, Cooper DN, Gitt MA, Leffler H: Galectins, structure and function of a large family of animal lectins. J Biol Chem 1994, 269:20807–20810
9. Gong HC, Honjo Y, Nangia-Makker P, Hogan V, Mazurak N, Bresalier RS, Raz A: The NH2-terminus of galectin-3 governs cellular compartmentalization and functions in cancer cells. Cancer Res 1999, 59:6239–6245
10. Ochieng J, Fridman R, Nangia-Makker P, Kleiner DE, Liotta LA, Stetler-Stevenson WG, Raz A: Galectin-3 is a novel substrate for human matrix metalloproteinases-2 and -9. Biochemistry 1994, 33:14109–14114
11. Nangia-Makker P, Sarvis R, Visscher DW, Bailey-Penrod J, Raz A, Sarkar FH: Galectin-3 and L1 retrotransposons in human breast carcinomas. Breast Cancer Res Treat 1998, 49:171–183
12. Lotz MM, Andrews Jr CW, Korzelius CA, Lee EC, Steele Jr GD, Clarke A, Mercurio AM: Decreased expression of Mac-2 (carbohydrate binding protein 35) and loss of its nuclear localization are associated with the neoplastic progression of colon carcinoma. Proc Natl Acad Sci USA 1993, 90:3466–3470

13. Strik HM, Deininger MH, Frank B, Schluesener HJ, Meyermann R: Galectin-3: cellular distribution and correlation with WHO-grade in human gliomas. J Neurooncol 2001, 53:13–20
14. Ellerhorst J, Troncoso P, Xu XC, Lee J, Lotan R: Galectin-1 and galectin-3 expression in human prostate tissue and prostate cancer. Urol Res 1999, 27:362–367
15. Pacis RA, Pilat MJ, Pienta KJ, Wojno K, Raz A, Hogan V, Cooper CR: Decreased galectin-3 expression in prostate cancer. Prostate 2000, 44:118–123
16. Ahmed H, Banerjee PP, Vasta GR: Differential expression of galectins in normal, benign and malignant prostate epithelial cells: silencing of galectin-3 expression in prostate cancer by its promoter methylation. Biochem Biophys Res Commun 2007, 358:241–246
17. Merseburger AS, Kramer MW, Hennenlotter J, Simon P, Knapp J, Hartmann JT, Stenzl A, Serth J, Kuczyk MA: Involvement of decreased galectin-3 expression in the pathogenesis and progression of prostate cancer. Prostate 2008, 68:72–77
18. Saggiorato E, Aversa S, Deandreis D, Arecco F, Mussa A, Puligheddu B, Cappia S, Conticello S, Papotti M, Orlandi F: Galectin-3: presurgical marker of thyroid follicular epithelial cell-derived carcinomas. J Endocrinol Invest 2004, 27:311–317
19. Miyazaki J, Hokari R, Kato S, Tsuzuki Y, Kawaguchi A, Nagao S, Itoh K, Miura S: Increased expression of galectin-3 in primary gastric cancer and the metastatic lymph nodes. Oncol Rep 2002, 9:1307–1312
20. Gillenwater A, Xu XC, el-Naggar AK, Clayman GL, Lotan R: Expression of galectins in head and neck squamous cell carcinoma. Head Neck 1996, 18:422–432
21. Nangia-Makker P, Raz T, Tait L, Hogan V, Fridman R, Raz A: Galectin-3 cleavage: a novel surrogate maker for matrix metalloproteinase activity in growing breast cancers. Cancer Res 2007, 67:11760–11768
22. Weiss RH: p21Waf1/Cip1 as a therapeutic target in breast and other cancers. Cancer Cell 2003, 4:425–429
23. Castronovo V, Van Den Brûle FA, Jackers P, Clausse N, Liu FT, Gillet C, Sobel ME: Decreased expression of galectin-3 is associated with progression of human breast cancer. J Pathol 1996, 179:43–48
24. van den Brule FA, Buicu C, Berchuck A, Bast RC, Deprez M, Liu FT, Cooper DN, Pieters C, Sobel ME, Castronovo V: Expression of the 67-kD laminin receptor, galectin-1, and galectin-3 in advanced human uterine adenocarcinoma. Hum Pathol 1996, 27:1185–1191
25. Shekhar MP, Nangia-Makker P, Tait L, Miller F, Raz A: Alterations in galectin-3 expression and distribution correlate with breast cancer progression: functional analysis of galectin-3 in breast epithelial-endothelial interactions. Am J Pathol 2004, 165:1931–1941
26. Van den Brûle FA, Waltregny D, Liu FT, Castronovo V: Alteration of the cytoplasmic/nuclear expression pattern of galectin-3 correlates with prostate carcinoma progression. Int J Cancer 2000, 89:361–367
27. Song YK, Billiar TR, Lee YJ: Role of galectin-3 in breast cancer metastasis: involvement of nitric oxide. Am J Pathol 2002, 160: 1069–1075
28. Bresalier RS, Mazurek N, Sternberg LR, Byrd JC, Yunker CK, Nangia-Makker P, Raz A: Metastasis of human colon cancer is altered by modifying expression of the beta-galactoside-binding protein galectin 3. Gastroenterology 1998, 115:287–296
29. Bresalier RS, Yan PS, Byrd JC, Lotan R, Raz A: Expression of the endogenous galactose-binding protein galectin-3 correlates with the malignant potential of tumors in the central nervous system. Cancer 1997, 80:776–787
30. Yang RY, Hsu DK, Liu FT: Expression of galectin-3 modulates T-cell growth and apoptosis. Proc Natl Acad Sci USA 1996, 93:6737–6742
31. Riss D, Jin L, Qian X, Bayliss J, Scheithauer BW, Young Jr WF, Vidal S, Kovacs K, Raz A, Lloyd RV: Differential expression of galectin-3 in pituitary tumors. Cancer Res 2003, 63:2251–2255
32. Hsieh TC, Wu JM: Changes in cell growth, cyclin/kinase, endogenous phosphoproteins and nm23 gene expression in human prostatic JCA-1 cells treated with modified citrus pectin. Biochem Mol Biol Int 1995, 37:833–841
33. Nangia-Makker P, Thompson E, Hogan C, Ochieng J, Raz A: Induction of tumorigenicity by galectin-3 in a non-tumorigenic human breast carcinoma cell line. Int J Oncol 1995, 7:1079–1087
34. Honjo Y, Nangia-Makker P, Inohara H, Raz A: Down-regulation of galectin-3 suppresses tumorigenicity of human breast carcinoma cells. Clin Cancer Res 2001, 7:661–668
35. Raz A, Zhu DG, Hogan V, Shah N, Raz T, Karkash R, Pazerini G, Carmi P: Evidence for the role of 34-kDa galactoside-binding lectin in transformation and metastasis. Int J Cancer 1990, 46:871–877
36. Ellerhorst JA, Stephens LC, Nguyen T, Xu XC: Effects of galectin-3 expression on growth and tumorigenicity of the prostate cancer cell line LNCaP. Prostate 2002, 50:64–70